The magnetic-field-driven effect of microwave detection in a manganite granular system

IOP PUBLISHING JOURNAL OF PHYSICS D: APPLIED PHYSICS

J. Phys. D: Appl. Phys. **41** (2008) 015004 (8pp) doi:10.1088/0022-3727/41/1/015004

The magnetic-field-driven effect of microwave detection in a manganite granular system

N V Volkov[1,2], E V Eremin[1], K A Shaykhutdinov[1], V S Tsikalov[1], M I Petrov[1], D A Balaev[1] and S V Semenov[1]

[1] Kirensky Institute of Physics, Siberian Branch, Russian Academy of Sciences, Krasnoyarsk 660036, Russia

[2] Siberian Federal University, Krasnoyarsk 660041, Russia

E-mail: volk@iph.krasn.ru

Received 31 August 2007, in final form 21 October 2007
Published 12 December 2007
Online at stacks.iop.org/JPhysD/41/015004

Abstract

We demonstrate the microwave detection effect in a granular $La_{0.7}Ca_{0.3}MnO_3$ sample. Dc voltage generated by the sample in response to microwave irradiation below the Curie temperature is found to be dependent on the applied magnetic field. The magnetic field dependence of the dc voltage has a broad peak resembling an absorption line. The detection effect depends substantially on the magnetic history of the sample; however, identical measurement conditions provide reproducibility of the experimental results. The detected dc voltage increases linearly with microwave power and strongly depends on a bias current through the sample. According to the results of systematic measurements, there exist two contributions to a value of the detected output signal. The first is magneto-independent; it can be explained in the framework of a mechanism used traditionally for description of the rectification effect in metal–insulator–metal junctions with nonmagnetic metals. The other is magneto-dependent; it originates from the interplay between the spin-dependent current through magnetic tunnel junctions and spin dynamics of the grains, which form these junctions in the sample.

1. Introduction

The phenomenon of the spin-dependent electron transport in magnetic tunnel structures has received close attention as the possible basis of a fundamentally new class of electronic devices [1]. Currently, two unique effects occurring in the magnetic tunnel structures are being thoroughly studied. They are the tunnel magnetoresistance (TMR) [2] and the spin-transfer torque (STT) effect [3] related to a torque exerted by the spin current on a local magnetic moment. The former allows controlling the electron current through a structure by the external magnetic field. The latter makes it possible to manipulate the magnetic state of a structure by the transport current. Indeed, in a number of experiments reported in the literature [4, 5] magnetization reversal of nanomagnets driven by the spin-polarized electrical current was observed. Moreover, the torque applied to a nanomagnet by the spin-polarized current provokes precession of its magnetic moment at microwave frequencies. At certain values of a steady current and static magnetic field, this precession excited by the spin transfer is persistent, and, consequently, may cause persistent microwaves with a frequency tuned by the current and external magnetic field [6]. In addition, the spin-transfer mechanism accounts for a reverse microwave effect, which consists of generation of the dc voltage across a nanometre-scale magnetic tunnel junction when a structure is externally irradiated with a microwave [7]. The microwave-frequency current due to the spin-torque effect excites an oscillation of nanomagnet magnetization under the resonance conditions, i.e. when the alternating current frequency coincides with a resonance frequency of the nanomagnet in the external magnetic field. This oscillation produces time-dependent resistance of the structure, which causes the effect of microwave detection.

It is not surprising that the observation of such unique and efficient phenomena in individual magnetic tunnel

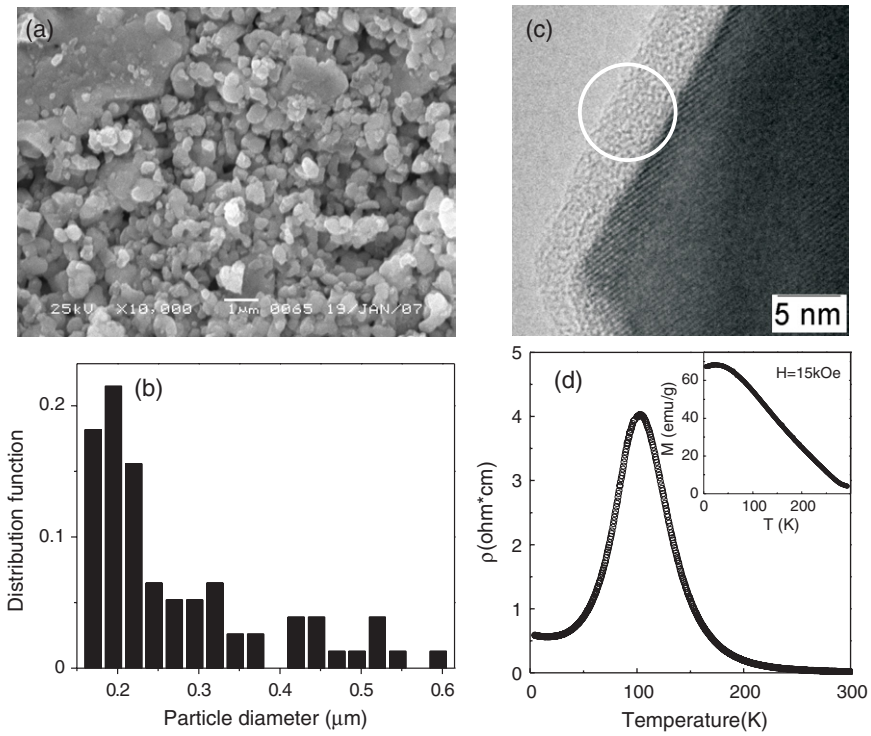

Figure 1. (*a*) SEM image of the $La_0.7Ca_0.3MnO_3$ polycrystalline sample. (*b*) Histogram showing the grain size distribution of the sample. (*c*) HRTEM image of a single grain. One can clearly see a pronounced surface layer (marked by the circle) of a grain, which is characterized by disorder of a high level. (*d*) Resistivity of the sample versus temperature. The inset shows the temperature dependence of magnetization of the sample.

junctions has stimulated intensive study of the effects of the spin-dependent electron transport in magnetic granular systems [8, 9]. The principal advantage of granular materials as systems, which involve a great number of ferromagnetic metallic grains separated by insulating boundaries, is the high density of magnetic tunnel junctions that may strengthen the electron spin-dependent effects. In addition, it is not improbable that the new effects typical of cooperative systems, i.e. the systems consisting of a great number of single-type elements, can be emerged. Indeed, it is well known that in complex systems under certain conditions the collectively ordered dynamical states can be revealed. The striking example is self-synchronizing oscillations in a large array of the interacting Josephson junctions [10]. Although observation of the spin-dependent electron transport in an explicit form is limited by technological difficulties of controlling the grain size and the spacing in the granular materials, by now the samples of granular systems with a huge TMR value are known [11, 12]. The presence of the TMR effect at room temperature in low magnetic fields makes these systems promising candidates for practical application. Some authors reported that the magnetoresistive properties of granular materials could be efficiently controlled via the selection of technology [13, 14]. The STT effect was also observed in magnetic granular solids [15, 16]. As was demonstrated, characteristics of this effect differ significantly from those previously observed in multilayers.

Here we demonstrate the magnetic-field-driven effect of microwave detection in a manganite granular system caused by coupling between the spin dynamics and spin-dependent electron transport. The choice of a material was conditioned by its half-metallic nature caused by a high degree of spin polarization of conduction electrons below the temperature T_C of the ferromagnetic transition [17]. By estimate, the spin polarization value in manganites may reach 100%. Therefore, the spin-dependent effects in manganite systems are expected to be more pronounced than those in the granular materials prepared from 3d-transition metals where spin polarization, as a rule, does not exceed 40%. Moreover, it is well established that a thin insulating layer inevitably forms on a grain surface of manganites due to high concentration of oxygen defects and faults [18]. Thus, the grains and their natural boundaries, which act as potential barriers between adjacent grains, create a vast array of tunnel junctions [19–21].

2. Experimental details

A polycrystalline $La_{0.7}Ca_{0.3}MnO_3$ sample was prepared from high-purity $La_2(CO_3)_3$, $CaCO_3$, and MnO_2 reagents by a conventional solid-state reaction, with a final sintering treatment for 24 h at 800 °C. The phase purity of the sample was checked with a Brucker D8 ADVANCE diffractometer. The powder x-ray diffraction patterns show that the sample has a single-phase perovskite-type structure without any impurity phase. The sample microstructure, i.e. the size and shape of grains and grain boundaries, was determined by an x-ray line broadening method, as well as by scanning and transmission electron microscopy (SEM and TEM, respectively). The SEM images show the abundance of nearly spherical particles (see figure 1(*a*)) whose size distribution is given as a histogram

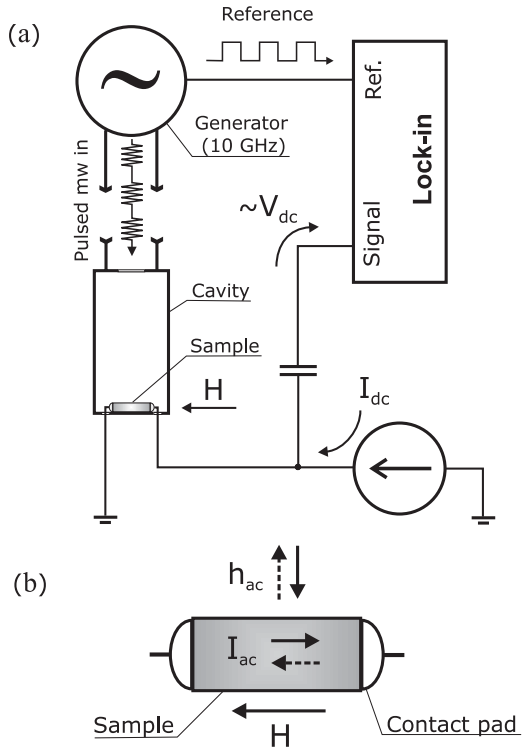

Figure 2. (*a*) A scheme of the circuit used for measurement of the microwave detection effect. (*b*) Experimental geometry: h_{ac} and j_{ac} denote microwave magnetic field and surface current patterns, respectively. In (*b*), the top view of the sample relative to (*a*) is presented.

in figure 1(*b*). It is seen that the average size of the particles is 0.20 μm, which is in close agreement with an x-ray diffraction result. The high-resolution TEM image (figure 1(*c*)) of a single grain clearly demonstrates its inner single-crystal nature and the presence of a disordered outer shell with an average thickness of 2 nm. Most likely, such grain boundaries, being insulating and nonmagnetic, form potential barriers between the neighbouring contacting grains. Indeed, large low-field magnetoresistance originating from the spin-polarized tunnelling of carriers across grain boundaries indicates the developed structure of the magnetic tunnel junctions in the sample.

Characterization resistivity measurements were performed using a standard four-probe configuration within the limits from 4.2 K to room temperature in the applied magnetic fields up to 80 kOe. Magnetization was determined with a vibrating sample magnetometer in the same temperature and field ranges. In figure 1(*d*), temperature dependences of resistivity and magnetization are presented. It is well known that the magnetic and transport properties of the polycrystalline and single-crystal manganites can substantially differ from each other, which is confirmed in our case. The mentioned difference is caused by the granular-like microstructure of the polycrystalline samples [18].

The experimental setup used for registration of the microwave detection effect is illustrated in figure 2. The sample in the form of a thin plate with two leads attached by silver epoxy is placed inside a microwave cavity operating at a frequency $f = 10$ GHz in the TE_{102} mode, as shown schematically in figure 2(*a*). To exclude an electric contact between the sample and the lower wall of the cavity, a thin dielectric film is used. The sample is located in the antinode of a high-frequency magnetic field h_{ac}, which induces a surface high-frequency current j_{ac} in the sample plane. The depth of the j_{ac} penetration into the sample depends on the resistivity and the magnetic permeability of the sample. The h_{ac} and j_{ac} patterns in the sample are given in figure 2(*b*). The j_{ac} direction coincides with the direction of the applied external magnetic field H as well as with the direction along which the detected dc voltage V_{dc} across the sample is measured.

The electric circuit described above permits application of a dc bias current I_{dc} through the sample during V_{dc} measurement. To measure the radiation-induced dc voltage across the sample only and to reduce noise, microwave irradiation is chopped at 1 kHz and the dc signal proportional to V_{dc} is recorded with the use of a lock-in amplifier. All the measurements of the microwave detection effect were performed in a helium cryostat in the temperature range from 4.2 to 300 K and the magnetic field range $-10\,\text{kOe} < H < 10\,\text{kOe}$.

Note that, along with epoxy glue, we used different materials of contact pads. In addition, different sample locations with the contact pads being outside the cavity were probed. The similarity of the results obtained in all the cases leads us to conclude that the microwave detection effect is independent of the contact phenomena and represents an intrinsic property of the sample itself.

3. Results

In figure 3 we plotted the dc voltage V_{dc} generated by the sample in response to microwave irradiation versus a magnetic field H. The dependences were obtained at different temperatures for the dc bias current $I_{dc} = 0$. For clarity, the curves are shifted by a certain offset. The inset in figure 3 shows the change in V_{dc} with temperature at $H = 0$ and the temperature dependence of the value $\Delta V_{dc} = V_{dc}(H_m) - V_{dc}(0)$, where H_m denotes the magnetic field corresponding to the maximum in the $V_{dc}(H)$ curves. The ΔV_{dc} value defines, in fact, a measure of sensitivity of the detection effect to the applied magnetic field. Generally, the detected dc voltage V_{dc} arises below 250 K. However, the pronounced effect of a magnetic field on the V_{dc} value becomes apparent at lower temperatures, below 180 K. The magnetic field dependence of V_{dc} has the shape of a broad peak resembling an absorption line. The strongest influence of a magnetic field is found around 100 K. With a further decrease in temperature, the peak spreads and becomes less distinct, which results in the ΔV_{dc} decreasing. Seemingly, there are two contributions to the V_{dc} value: the dc voltage response independent of a magnetic field and the additional part of the signal which can be controlled by the applied magnetic field. From our point of view, this response is the magneto-dependent response, which is of the most interest.

The systematic measurements showed that the behaviour of V_{dc} versus H depends considerably on the magnetic history of the sample, i.e. on the value and direction of the magnetic

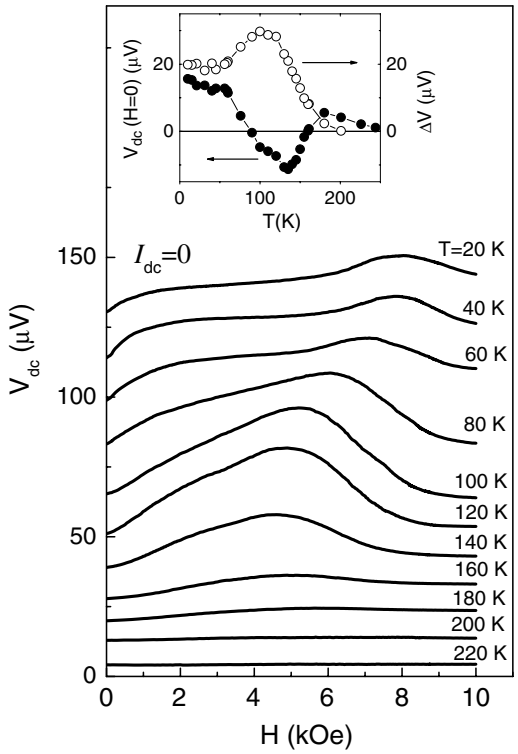

Figure 3. The detected dc voltage V_{dc} as a function of magnetic field at a bias current $I_{dc} = 0$; the dependences measured at different temperatures are shown. For clarity, the curves are shifted by a constant offset. Inset: the temperature dependences of the detected voltage at $H = 0$, $V_{dc}(H = 0)$ and $\Delta V_{dc} = V_{dc}(H_m) - V_{dc}(0)$ where H_m is the magnetic field corresponding to the maximum in the $V_{dc}(H)$ curves.

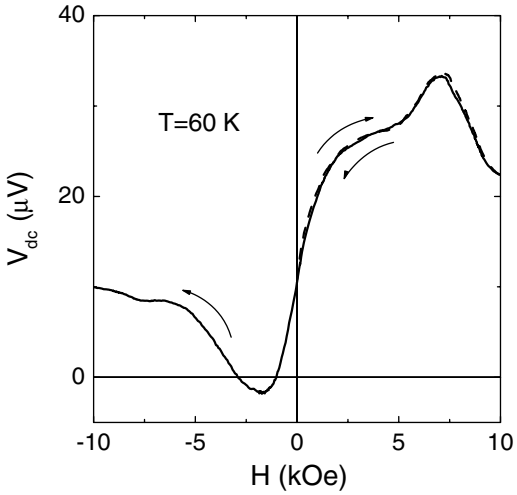

Figure 4. The detected dc voltage V_{dc} as a function of the magnetic field cycling first from zero to the maximum positive value and then to the maximum negative value as indicated by the arrows; the bias dc current through the sample is $I_{dc} = 0$; the measurement temperature is 60 K.

field at which the sample is cooled down. At zero-field cooling the magneto-dependent contribution to the detected signal was weakly measurable and reproducibility of the results was lacking. We obtained the maximal effect using the following procedure: the sample was cooled in a magnetic field of 10 kOe directed transversely to the measuring field, while the dependences of V_{dc} on H were recorded in a heating mode. All the experimental data presented were obtained just under these conditions. Such a procedure provides reproducibility of the measurement results. The strong dependence of the detection effect on the magnetic state of the sample was revealed upon inversion of the applied magnetic field. Figure 4 shows that the reverse sweeping of the magnetic field from a high value to zero does not change the $V_{dc}(H)$ dependence, whereas the inversion of a magnetic field sign provokes principal changes in the $V_{dc}(H)$ curve. One can clearly see that magnetization reversal changes the sign of the magneto-dependent contribution to the detected voltage and the shape of the $V_{dc}(H)$ curve.

In figure 5(*a*), the typical V_{dc} versus magnetic field curves recorded at different levels of microwave power P_{mw} are shown. We used these data to plot the power dependences of $V_{dc}(H = 0)$ and the ΔV_{dc} value; the former dependence is associated with the magneto-independent contribution to the detected voltage, while the latter characterizes the contribution depending on the applied magnetic field. It is seen from figure 5(*b*) that both $V_{dc}(0)$ and ΔV_{dc} increase linearly with P_{mw}/P_{mw}^{max} ($P_{mw}^{max} = 10$ mW), which means that the sample behaves like a square-law detector regardless of whether the magneto-independent or magneto-dependent contribution to the detected voltage is taken into consideration.

Next, we studied the effect of a bias current I_{dc} through the sample on the dc voltage generated in response to microwave irradiation. Figure 6(*a*) shows the V_{dc} versus magnetic field curves obtained for several I_{dc} values. The V_{dc} value strongly increases with I_{dc} until the saturation current reaches about 2 mA, while the shape of the $V_{dc}(H)$ curves is not appreciably affected by the bias current. As I_{dc} increases from 0 to 2 mA, the detected output grows on average by a factor of 20. Figure 6(*b*) demonstrates the evolution of the detected voltages $V_{dc}(H = 0)$ and ΔV_{dc} as the current I_{dc} through the sample increases. It should be noted that in both cases the detected output first increases with I_{dc} and then saturates at about the same value of the bias current, but the low-current ($I_{dc} < 2$ mA) behaviors of the output in the first and second cases are substantially different. Apparently, the latter may indicate the different origin of the magneto-independent and the magnetic-field-driven contributions to the dc voltage generated by the sample in response to microwave irradiation.

4. Discussion

It is obvious that the polycrystalline sample under study is a remarkably complex granular system, which is characterized by a wide distribution of grain sizes and shapes. Since grains possess the core-shell structure (ferromagnetic cores with the metallic-type conductivity coated with thin insulating nonmagnetic shells), they form a strongly inhomogeneous, randomly distributed network of magnetic tunnel junctions in the sample. The microstructure of the sample influences the static and dynamic magnetic properties of the system. First of all, nonmagnetic grain boundaries significantly weaken the magnetic coupling between grains; the widely spread ferromagnetic transition observed in the sample indicates the

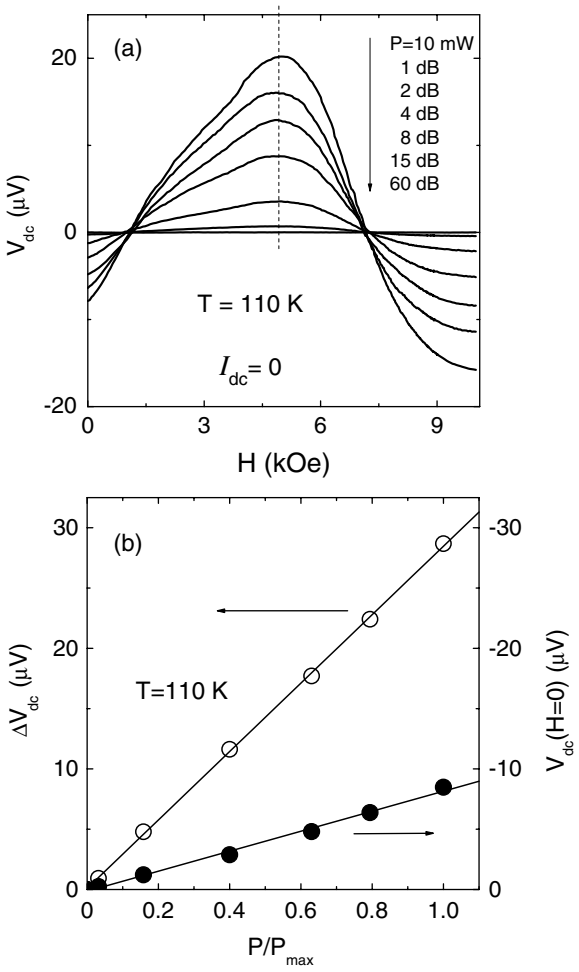

Figure 5. (*a*) The detected dc voltage V_{dc} as a function of the magnetic field measured at different levels of microwave power at a temperature of 110 K and the dc bias current through the sample $I_{dc} = 0$. (*b*) The dependences of the detected voltage $V_{dc}(H = 0)$ and the $\Delta V_{dc} = V_{dc}(H_m) - V_{dc} = 0$ value on microwave power; H_m is the magnetic field corresponding to the maximum in the $V_{dc}(H)$ curves.

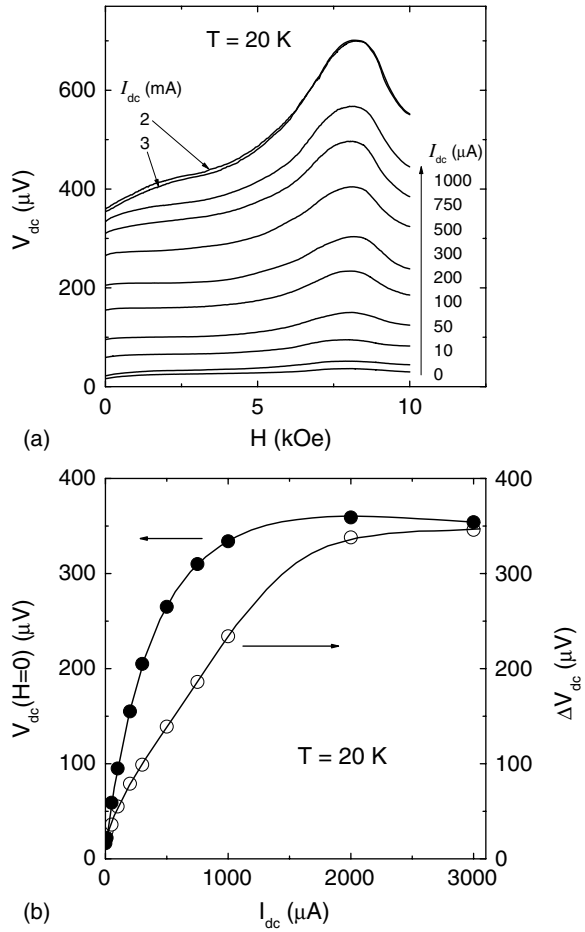

Figure 6. (*a*) The detected dc voltage V_{dc} as a function of the magnetic field measured at different values of the bias current at temperature 20 K. (*b*) The dependences of the detected voltage $V_{dc}(H = 0)$ and the $\Delta V_{dc} = V_{dc}(H_m) - V_{dc}(0)$ value on bias current through the sample I_{dc}; H_m is the magnetic field corresponding to the maximum in the $V_{dc}(H)$ curves.

distribution of values of this coupling. In fact, each crystallite in the sample is in a characteristic effective magnetic field determined by the inter-grain interactions, crystallographic anisotropy, demagnetizing fields and external magnetic field. This leads to the difference in the magnetization processes and distributions of ferromagnetic resonance fields of individual crystallites.

Nevertheless, we believe that the detection mechanisms in granular materials may be illustrated qualitatively by an example of single tunnel transitions. Actually, the detection effect in the system we investigated may be understood by attracting a classical model of the voltage rectification in a tunnel junction [22]. A tunnel junction formed by two metal electrodes with a thin insulating barrier between them (the M–I–M structure) possesses the nonlinear voltage–current characteristic and, thereby, can cause the rectification of the high-frequency current flowing through the structure. In the case of a granular system, the dc voltage generated by the sample is a total response of the set of tunnel junctions to the high-frequency current induced by microwave irradiation. All the experimentally observed peculiarities in the behaviour of V_{dc}, in particular, polarity reversal with temperature at $I_{dc} = 0$, can be attributed to the geometrical asymmetry of the junctions, nonidentity of the junction electrodes and the distribution of characteristics of the tunnel junctions in a sample [23, 24].

At the same time, the mechanism, which is traditionally used to describe the detection effect in the M–I–M structures, does not help to explain the strong dependence of the effect on magnetic field. We suppose that in this case we should consider the spin-dependent electron tunnelling, which has to develop inevitably in the tunnel junctions with ferromagnetic electrodes. Let us recall that the magneto-dependent contribution to V_{dc} for the sample under study arises only at temperatures below T_C, when the high degree of spin polarization is realized in the manganite materials, and the enhanced spin-dependent transport phenomena should take place in the structures involving these materials. Below we suggest a mechanism, which may be responsible for the magneto-dependent contribution to the detected voltage in the magnetic tunnel junctions. The mechanism is based on the interplay between the spin dynamics and spin-dependent transport. The principal details of the mechanism

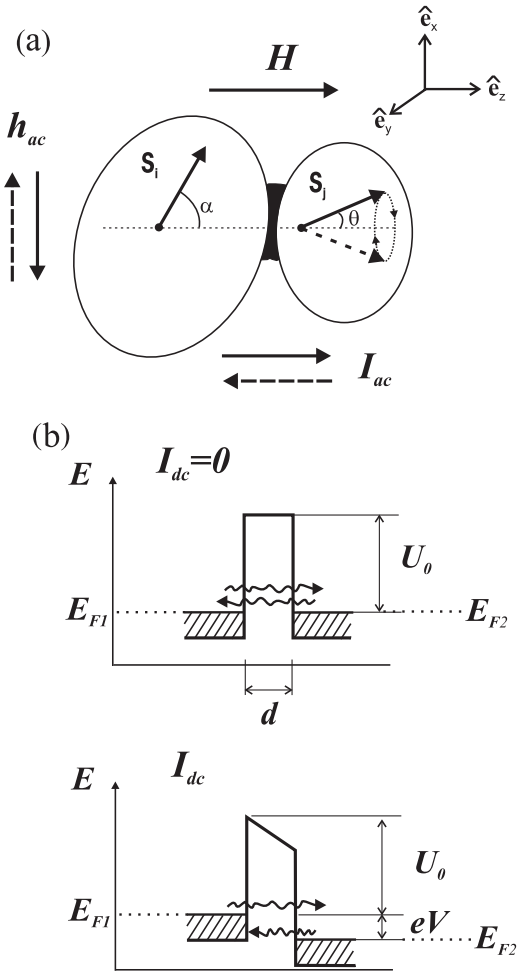

Figure 7. (*a*) The schematic of adjacent magnetic grains in the sample. The arrows $\hat{\boldsymbol{s}}_i$ and $\hat{\boldsymbol{s}}_j$ indicate the unit vectors along magnetization of the ith and jth grains; $\hat{\boldsymbol{s}}_i$ has a fixed direction, but $\hat{\boldsymbol{s}}_j$ is under resonance conditions and oscillates at a frequency f around the magnetic field direction. (*b*) The sketch representing a change in the energetic structure of the junction resulting from the bias.

can be clarified by an example of an individual magnetic tunnel junction formed by two adjacent ferromagnetic grains separated by a thin insulating boundary. In figure 7, the sketch of such a junction along the current path is presented. As mentioned above, each of the grains possesses the characteristic effective magnetic field, therefore, the behaviour of magnetization and magnetic resonance conditions should differ for different grains. Let us assume that at a certain value of the external magnetic field directed along the current path the magnetic moment of the ith grain is pinned at an angle of α relative to the direction of the applied field, whereas the jth grain is under resonance conditions, and its moment oscillates at a frequency f around the magnetic field direction. This oscillation produces the time-dependent resistance of the magnetic tunnel junction, which can be expressed as

$$R(t) = R_{\uparrow\uparrow} + \frac{\Delta R}{2}(1 - \hat{\boldsymbol{s}}_i \cdot \hat{\boldsymbol{s}}_j). \qquad (1)$$

Here $\hat{\boldsymbol{s}}_i$ and $\hat{\boldsymbol{s}}_j$ are the unit vectors along magnetization of the ith and jth grains, respectively; the equilibrium direction of $\hat{\boldsymbol{s}}_i$ is determined by $\hat{\boldsymbol{s}}_i = (\hat{\boldsymbol{e}}_x \cos\phi + \hat{\boldsymbol{e}}_y \sin\phi)\sin\alpha + \hat{\boldsymbol{e}}_z \cos\alpha$ (ϕ is the angle between the $\hat{\boldsymbol{s}}_i$ projection onto the xy-plane and $\hat{\boldsymbol{e}}_x$), but $\hat{\boldsymbol{s}}_j$ oscillates as $\hat{\boldsymbol{s}}_j = (\hat{\boldsymbol{e}}_x \cos(2\pi f t) + \hat{\boldsymbol{e}}_y \sin(2\pi f t))\sin\theta + \hat{\boldsymbol{e}}_z \cos\theta$ (θ is the precession angle); $R_{\uparrow\uparrow}$ is the resistance of the junction when $\hat{\boldsymbol{s}}_i$ and $\hat{\boldsymbol{s}}_j$ are parallel, $\Delta R = R_{\uparrow\downarrow} - R_{\uparrow\uparrow}$ is the resistance increase when $\hat{\boldsymbol{s}}_i$ and $\hat{\boldsymbol{s}}_j$ are antiparallel. Considering that the high-frequency magnetic field $h_{\rm ac}$ induces the high-frequency current $I(t) = I_{\rm ac}\sin(2\pi f t - \delta)$ (δ is the possible phase shift between the oscillating $\hat{\boldsymbol{s}}_j$ and I) passing through the junction, the voltage $V(t) = I(t)R(t)$ will contain a term involving mixing between $I_{\rm ac}$ and $\Delta R(t)$, and thus the rectified voltage will be

$$V_{\rm dc} = \langle I(t)R(t)\rangle_T = \frac{I_{\rm ac}\Delta R}{4}\sin\theta\,\sin\alpha\,\cos(\phi - \delta). \qquad (2)$$

Figure 7 makes it easier to interpret qualitatively the rectification mechanism based on the spin-transfer phenomenon. Indeed, let us assume for simplicity that $\phi - \delta = 0$; then the resistance for the spin current flowing from the ith to jth grain is lower due to a smaller angle between $\hat{\boldsymbol{s}}_i$ and $\hat{\boldsymbol{s}}_j$; however, for the opposite direction of the alternating current, the resistance is higher, owing to a larger angle. This mechanism of the microwave detection is similar to that proposed by Tulapurkar *et al* [7] to explain the diode effect in a single magnetic tunnel junction. There is, however, a notable difference: in their case, the resonance oscillation of magnetization in the electrode of the junction is excited by a high-frequency spin-polarized current passing through the junction, while in our case, the oscillation is caused by a magnetic microwave field.

Certainly, for the random network of magnetic tunnel junctions implemented in a granular system the physical picture would be more complicated. The magnetic tunnel junctions are not identical, and the differences in their characteristics are described by certain distribution functions. First and foremost, the $V_{\rm dc}$ behaviour versus magnetic field is defined by a distribution function for the resonance fields of individual grains in the system. Thus, the spread of the peak-like $V_{\rm dc}(H)$ dependence at low temperature is related to the growth of magnetization and anisotropy fields of individual grains that results in a wider spread in the values of the resonance field of grains in the sample. This conclusion is consistent with data of the magnetic resonance measurements we carried out on our sample. The spectra obtained exhibit substantial broadening of the magnetic resonance signal below about 100 K. Since the broadening is more gradual in the case of single crystals, we can attribute the linewidth behaviour anomaly to the spread in values of the resonance fields of individual grains.

Further, the distribution of grain magnetizations in the ϕ angle for a statistical set is expected to be symmetrical for an arbitrary α value and a fixed δ value. Consequently, the summation of the rectified voltages over all the tunnel junctions in the system should result in the zero magneto-dependent contribution to $V_{\rm dc}$ for the entire sample. For the magnetic-field-driven part of $V_{\rm dc}$ to be nonzero, the angle distribution of grain magnetization should be asymmetrical. In our case, such an asymmetrical distribution is provided by the difference in coercive fields of individual grains and

magnetic history of the sample (cooling in a magnetic field of the preferential direction). The pronounced hysteretic behaviour of the magnetization versus magnetic field indicates that the asymmetry in the distribution of grain magnetization is actually realized in our sample under the field-cooling conditions selected. The changes in the sign of the effect and the shape of the $V_{dc}(H)$ curve when a magnetic field is inverted in sign (see figure 4) indicate the change either in the magnetization distribution of the grains forming magnetic tunnel junctions or in the set of the junctions involved in a rectification process upon magnetic reversal.

Let us consider the power behaviour of the detected output voltage. According to the proposed model, the magneto-dependent contribution to V_{dc} should depend linearly on microwave irradiation power; in other words, the sample should behave like a square-law detector, $V_{dc} \sim h_{ac}^2$. Indeed, each of the I_{ac} and $\sin\theta$ values in (2) is directly proportional to h_{ac}, although, in the latter case, it is valid only at low power levels. Figure 5(*b*) shows that in our sample the magneto-dependent contribution to V_{dc} increases linearly with an increase in microwave power. The power dependence of $V_{dc}(H = 0)$ presented in the same plot is also linear. The latter is the expected result if the magneto-independent part of V_{dc} is defined by the classical rectification mechanism in M–I–M junctions, since, in this case, the detected output voltage is $V_{dc} \sim I_{ac}^2$ at a low power level of microwave irradiation [22].

As for the influence of the bias current on the detected dc voltage, we suppose that the I_{dc} effect on a V_{dc} value may be explained using a model of elastic tunnelling through the M–I–M junction with nonmagnetic electrodes [22]. An increase in I_{dc} causes the lowering of the Fermi level of one electrode relative to the other by a value eV_b, where V_b is the corresponding bias voltage across the junction (see figure 7(*b*)). This results in the tunnelling asymmetry, i.e. the difference in resistivity of the junction for the forward and backward currents (R_F and R_B, respectively). Then the detected dc voltage for a single junction can be expressed as $V_{dc} = \langle I(V(t)t)R\rangle_T = \int_0^{\pi} I_{ac}\sin(2\pi ft)R_F\mathrm{d}(2\pi ft) - \int_{\pi}^{2\pi} I_{ac}\sin(2\pi ft)R_B\mathrm{d}(2\pi ft)$. In the low-voltage limit, an increase in the bias across a junction enhances the difference between R_F and R_B, which causes amplification of the dc output voltage. The total bias dependences of R_F and R_B are determined by the electronic structure of the metallic electrodes and the barrier parameters. In general, the experimental dependences of V_{dc} on I_{dc} obtained for our sample at $H = 0$, where the classical model of rectification is apparently valid, exhibit a behaviour similar to that of the dependences calculated for a single junction on the basis of a free-electron model of metals [23]. We believe that the approach described here can be applied to the analysis of the magneto-dependent V_{dc} part at the increasing of the bias current through a sample. By analogy with the classical model, the tunnelling asymmetry arising due to the bias can be formally taken into account assuming $R_{\uparrow\uparrow}$, $R_{\uparrow\downarrow}$ and, hence, ΔR in (1) to be dependent on a direction of the high-frequency current in a junction. At the same time, the difference in the behaviours of $V_{dc}(H = 0)$ and ΔV_{dc} versus I_{dc} (see figure 6(*b*)) implies that the mechanisms responsible for the magneto-dependent and magneto-independent contributions to the detected voltage may differ in origin. We should note here that the magneto-independent contribution to V_{dc} is determined by a complete set of the tunnel junctions in the system, while, in accordance with the proposed mechanism, only the limited and strictly defined set of the junctions can contribute to the magnetic-field-driven part of V_{dc}. It is possible that the difference in behaviours of V_{dc} at $H = 0$ and ΔV_{dc} is related to this fact.

5. Conclusion

We have observed the effect of microwave-frequency detection in the polycrystalline $La_{0.7}Ca_{0.3}MnO_3$ sample. The examined sample is a granular system consisting of ferromagnetic grains with the metallic conductivity coated with nonmagnetic insulating layers. Such a pattern implies the formation of a set of magnetic tunnel junctions in the sample. At these junctions the rectification of the high-frequency alternating current induced by a magnetic microwave field occurs. The detected dc voltage across the sample can be presented as the sum of two contributions, one being magnetically independent and the other being dependent on the external magnetic field. We suppose that the first contribution can be explained in the framework of a mechanism, which is traditionally used for the description of the rectification effect at metal–insulator–metal junctions with nonmagnetic metals. As for the magneto-dependent contribution, we propose a mechanism based on the interplay between the spin-dependent current through the magnetic tunnel junctions and the spin dynamics of the grains forming these junctions in the sample.

Acknowledgments

This study was supported by the KRSF-RFBR 'Enisey2007', Grant No 07-02-96801-a and the Division of Physical Sciences of RAS, Program 'Spin-dependent Effects in Solids and Spintronics', and Project No 2.4.2 of the SB RAS. NV and KS also thank the Russian Science Support Foundation.

References

[1] Zutic I, Fabian J and Das Sarma S 2004 *Rev. Mod. Phys.* **76** 323
[2] Barthelemy A *et al* 2002 *J. Magn. Magn. Mater.* **242–245** 68
[3] Waintal X and Parcollet O 2005 *Phys. Rev. Lett.* **94** 247206
[4] Sun J Z 1999 *J. Magn. Magn. Mater.* **202** 157
[5] Huai Y, Albert F, Nguyen P, Pakala M and Valet T 2004 *Appl. Phys. Lett.* **84** 3118
[6] Sun J 2003 *Nature* **425** 359
[7] Tulapurkar A A, Suzuki Y, Fukushima A, Kubota H, Maehara H, Tsunekawa K, Djayaprawira D D, Watanabe N and Yuasa S 2005 *Nature* **438** 339
[8] Yakushiji K, Mitani S, Takanashi K and Fujimori H 2002 *J. Phys. D: Appl. Phys.* **35** 2422
[9] Zeng H, Black C T, Sandstrom R L, Rice P M, Murray C B and Sun S 2006 *Phys. Rev.* B **73** R020402
[10] Benz S P and Burroughs C J 1991 *Appl. Phys. Lett.* **58** 2162
[11] Chen P, Xing D Y, Du Y W, Zhu J M and Feng D 2001 *Phys. Rev. Lett.* **87** 107202
[12] Akinaga H 2002 *J. Magn. Magn. Mater.* **239** 145
[13] Rivas J, Hueso L E, Fondado A, Rivadulla F and Lopez-Quintela M A 2000 *J. Magn. Magn. Mater.* **221** 57

[14] Roy B, Poddar A and Das S 2006 *J. Appl. Phys.* **100** 104318
[15] Chen T Y, Huang S X, Chien C L and Stiles M D 2006 *Phys. Rev. Lett.* **96** 207203
[16] Pallecchi I, Pellegrino L, Caviglia A, Bellingeri E, Canu G, Gazzadi G C, Siri A S and Marre D 2006 *Phys. Rev.* B **74** 014434
[17] Viret M, Drouet M, Nassar J, Contour J P, Fermon C and Fert A 1997 *Europhys. Lett.* **39** 545
[18] Dey P and Nath T K 2006 *Phys. Rev.* B **73** 214425
[19] Balcells L, Martinez B, Sandiumenge F and Fontcuberta J 2000 *J. Magn. Magn. Mater.* **211** 193
[20] Dutta A, Gayathri N and Ranganathan R 2003 *Phys. Rev.* B **68** 054432
[21] Niebieskikwiat D, Sanchez R D, Lamas D G and Caneiro A 2003 *J. Appl. Phys.* **93** 6305
[22] Kwok S P, Haddad G I and Lobov G 1971 *J. Appl. Phys.* **42** 554
[23] Miskovsky N M, Shepherd S J, Gutler P H, Sullivan T E and Lucas A A 1979 *Appl. Phys. Lett.* **35** 560
[24] Van der Heijden R W, Jansen A G M, Stoelinga J H M, Swartjes Y M and Wyder P 1980 *Appl. Phys. Lett.* **37** 245